Modeling and Simulation of Micromachined Gyroscopes in The Presence of Imperfections

A. Shkel*, R.T. Howe** and R. Horowitz***

* EECS Dept./BSAC, 497 Cory Hall, UC-Berkeley. ashkel@eecs.berkeley.edu
** EECS Dept./BSAC, 231 Cory Hall Rm. 1770, UC-Berkeley. howe@eecs.berkeley.edu
***ME Dept./BSAC, 5138 Etcheverry Hall, UC-Berkeley. horowitz@me.berkeley.edu

ABSTRACT

This paper studies behavior of non-ideal vibratory micromachined gyroscopes. The use of methods of motion decomposition [1] is the essence of the proposed analytical approach. The method is based on partitioning the equations of motion on fractions which are changing in different time scales. The approach allows rapid simulation of the long-term response of the gyroscope in presence of imperfections. The central result of the paper is the classification of errors in accordance with their influence on the gyroscope behavior.

Keywords: micromachined gyroscopes, fabrication defects, anisoelasticity, damping, motion decomposition

INTRODUCTION

Difficulties of full-time scale simulation of vibratory gyroscopes are often acknowledged, but has never received enough attention in the literature. The major challenge simulating these systems is the existence of multiple time-scales: one is defined by the natural frequency of the gyroscope (in kHz range), the other - by the input angular velocity (ranging between degrees per second and sub-degrees per hour). These two time scales differ by more than 4-6 orders of magnitude. Straightforward plug-in of the equations of motion into one of the numerical integration packages (for example, MATLAB) will simulate the behavior of the system in the fastest time-scale. However, when the effect of manufacturing defects or system response to control actions are examined, we are interested in the long-term behavior of the system, which is of the order of the input angular velocity. Thus, direct substitution of governing equations into the simulation package is computationally impractical. In this paper we propose an approach for overcoming these difficulties.

Fabrication imperfections are a major factor limiting the performance of micromachined gyroscopes. Understanding of the behavior of gyroscopes in presence of imperfections and ability to control and compensate for defects are essential for improving its performance. All micromachined gyroscopes are planar vibratory mechanical structures fabricated primarily from polysilicon or single crystal silicon. Common processing techniques that are used to sculpt structures include bulk micromachining, wafer-to-wafer bonding, surface micromachining, and high-aspect ratio micromachining. Each of these fabrication processes involves multiple processing steps including the deposition, etching, and patterning of materials. Depending on the technology, different number of steps is involved and different tolerance can be achieved. As a rule, every fabrication step contribute to imperfections in the gyroscope. In practice, imperfections are reflected in asymmetry and anisoelasticity of the structure. Consequently, asymmetries result in undesirable constantly acting perturbations in the form of mechanical and electrostatic forces.

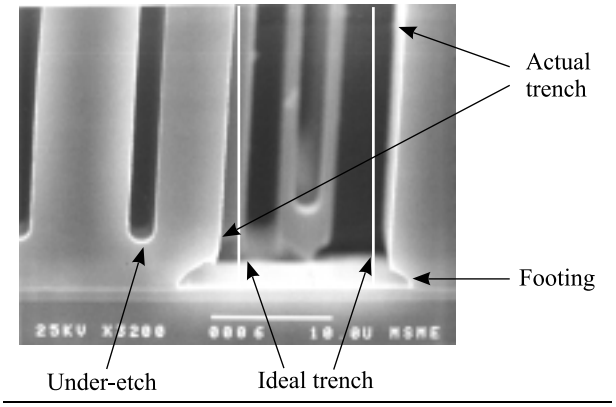

Figure 1: Examples of typical fabrication imperfections in "bulk" micromachined gyroscopes. With the deep-reactive-ion-etching (DRIE) vertical sidewalls can be produced with the accuracy of approximately 2 degrees; footing and under-etch are potentially a problem due to aspect ratio etching variation. Photo courtesy of BSAC.

Apparently, vibratory gyroscopes are equally sensitive not only to measured physical phenomena - the Coriolis force, but also to undesirable perturbations and defects. The objective of this paper is to take a look into several cases of imperfections which are of practical interest, illustrate the effect of imperfections, and propose a method for analysis of non-ideal gyroscopes.

MODELING OF IMPERFECTIONS

The governing equations in Cartesian coordinates of a non-ideal gyroscope are given by

$$\ddot{X} + \omega_n^2 X - 2\Omega\dot{Y} = (\omega_n^2 - \omega_x^2)X + c_{xy}Y + d_{xx}\dot{X} + d_{xy}\dot{Y}$$
$$\ddot{Y} + \omega_n^2 Y + 2\Omega\dot{X} = (\omega_n^2 - \omega_y^2)X + c_{yx}X + d_{yy}\dot{Y} + d_{yx}\dot{X}$$

The terms on the right-hand side represent potential sources of error which can be viewed as external perturbations of the ideal system. The coefficients multiplying the position variables represent non-ideal spring forces that could arise, for example, from the lack of perfect symmetry in the device. They may be collectively identified as "anisoelasticity". The terms multiplying the velocity variables are damping terms and could represent losses in the system due to various physical causes such as structural damping, transmission of energy to suspension, etc.

The left-hand side of the governing equations models an ideal vibratory gyroscope with matched natural frequencies ω_n. The essential feature of these equations is the presence of the Coriolis acceleration terms $-2\Omega\dot{Y}$ and $2\Omega\dot{X}$. These two terms will appear only if the equation of motion are written in a non-inertial coordinate frame. It is the Coriolis acceleration that causes a transfer of energy between two of the gyro's modes of operation (Figure 2).

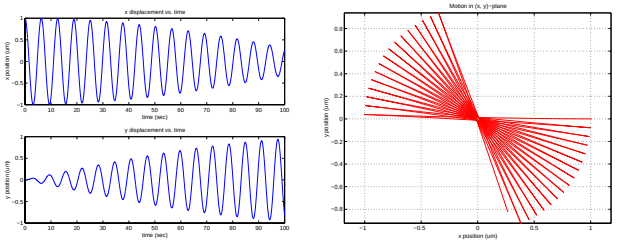

(a) (b)

Figure 2: The Coriolis acceleration causes the precession of the gyroscope's line of oscillation. The oscillating proof mass is trying to keep the line of oscillation constant in the inertial space; in a non-inertial coordinate frame, this is observed as the transfer of energy between two of the gyro's modes of operation.

If the "input" angular velocity Ω is zero, and under appropriate initial conditions, the ideal gyroscope will oscillate along a straight line. The orientation of the straight line is defined by initial conditions. In a more general case, when the initial conditions are such that the vector of displacement is not parallel to the vector of velocity, the orbit of the gyro motion is an ellipse. This observation is important for interpreting the results of testing and identification of imperfections in micromachined gyroscopes.

Frequency Mis-Match and Anisoelasticity

The most common and easily observed imperfections in micromachined gyroscopes are frequency mis-match and anisoelasticity. Analysis of gyroscopes in presence of these imperfections does not require any special treatment and can be done using the eigenvalue analysis [2]. When there is no input rotation and only anisoelasticity is present, the equations of motion have the form

$$\begin{bmatrix} \ddot{X} \\ \ddot{Y} \end{bmatrix} + \begin{bmatrix} \omega_x^2 & c_{xy} \\ c_{xy} & \omega_y^2 \end{bmatrix} \cdot \begin{bmatrix} X \\ Y \end{bmatrix} = 0$$

The eigenvectors of this system define a pair of principal (cardinal) elastic axes that define stable directions of a straight line motion of the gyroscope (see Figure 3).

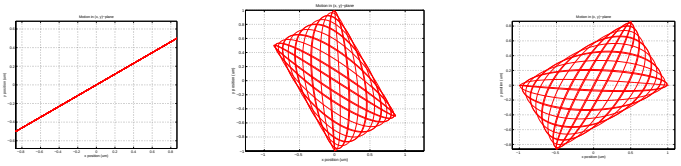

(a) (b) (c)

Figure 3: (a) If the motion starts along a principal elastic axis it will remain on a straight line; (b),(c) if the motion starts out of a principal axis it does not remain on a straight line; depending on the initial conditions the oscillation will be in one of the attraction regions defined by principal elastic axes.

Next we show the connection between the elements of the stiffness matrix and the main axes of elasticity. Assume that the axis of symmetry of the ideal (defect-free) gyroscope are X and Y (Figure 4). Due to imperfections in fabrication the X and Y axes may not coincide with the principal axis of elasticity $\underline{X}$ and $\underline{Y}$. Then, the stiffness matrix in {X,Y} coordinate frame has the form

$$K = \begin{bmatrix} k_{xx} & k_{xy} \\ k_{yx} & k_{yy} \end{bmatrix}, \quad k_{xy} = k_{yx} \quad \text{and} \quad k_{ij} = M c_{ij} \qquad (1)$$

Assume that the principal spring axes are tilted by an angle α from the reference coordinate system (Figure 4). Also, assume that the principal spring constants are K_1 and K_2 ($K_1 > K_2$). Then elements of the stiffness matrix (1) can be presented in terms of K_1, K_2, and α as follows

$$\begin{aligned} k_{xx} &= \frac{K_1 + K_2}{2} + \frac{K_1 - K_2}{2}\cos(2\alpha) \\ k_{yy} &= \frac{K_1 + K_2}{2} + \frac{K_2 - K_1}{2}\cos(2\alpha) \\ k_{xy} &= k_{yx} = \frac{K_1 - K_2}{2}\sin(2\alpha) \end{aligned} \qquad (2)$$

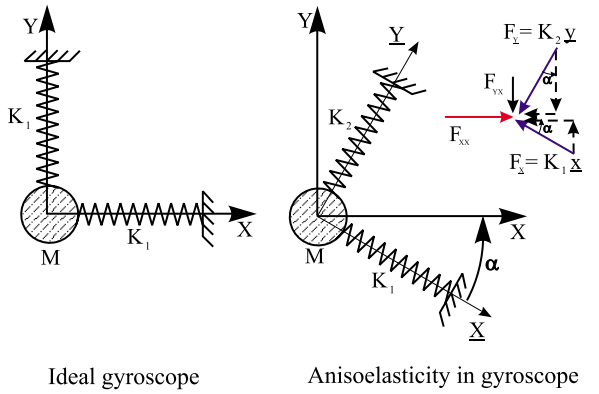

Figure 4: Imperfections result in mis-alignment of the main axes of elasticity with intended structural axes of symmetry

Derivation of (2) is illustrated in Figure 4.

By analogy with stiffness, damping can also be described in terms of two main axes of damping. In general, the principal axes of elasticity and damping are not necessarily aligned because asymmetry in stiffness and damping are caused by different physical phenomena. The location of the principal axis of damping and the magnitude of the damping difference are determined by an averaging of the damping asymmetries. By analogy with stiffness, damping matrix D can be written as a function of principal damping constants D_1, D_2 and the angle of axes orientation β. It has the form

$$\begin{bmatrix} \frac{D_1+D_2}{2} + \frac{D_1-D_2}{2}\cos(2\beta) & \frac{D_1-D_2}{2}\sin(2\beta) \\ \frac{D_1-D_2}{2}\sin(2\beta) & \frac{D_1+D_2}{2} + \frac{D_2-D_1}{2}\cos(2\beta) \end{bmatrix}$$

Damping asymmetry, like damping itself, arises principally from asymmetry in aerodynamic drag, structural damping, transmission of energy to the suspension, etc. Major damping mechanisms involved in the vibratory gyroscope include viscous damping of the ambient air (Stoke's damper) and the air layer between the proof-mass and the substrate (slide film damper) [3].

MOTION DECOMPOSITION

The application of the method of motion decomposition (or fractional analysis [1]) includes three steps. First we introduce the characteristic parameters of the system. This is followed by a non-dimensional analysis with respect to the chosen time-scale and identification of the small parameters of the system. The decomposition procedure is concluded by the averaging of the system with respect to the time scale of interest. The application of this method to vibratory gyroscopes allows rapid simulation of the long-term response of the gyroscopes to the constantly acting perturbations (e.g., due to fabrication imperfections). Details of the procedure can be found in [1], [4].

Due to space limitations, we skip details of the dimensional analysis, and just present the equations of motion with perturbations in non-dimensional form:

$$\begin{aligned} \ddot{x}_1 + x_1 &= \varepsilon Q_1(t, x, \dot{x}) \\ \ddot{x}_2 + x_2 &= \varepsilon Q_2(t, x, \dot{x}),\ \varepsilon \sim \frac{\Omega}{\omega_n} \ll 1 \end{aligned} \qquad (3)$$

Here $x = (x_1, x_2)$ is a non-dimensional displacement, Q_1 and Q_2 are constantly acting perturbations including the Coriolis force, ε is a small non-dimensional parameter defined by characteristic values of the system.

Below we use the procedure described in [1] to convert the system (3) to the standard form (6). The first step of the procedure is to find a non-perturbed solution of the system (3), i.e. when $\varepsilon = 0$. In this case, the solution is

$$\begin{aligned} x_1 &= C_1\cos t + C_3\sin t, \quad \dot{x}_1 = -C_1\sin t + C_3\cos t, \\ x_2 &= C_2\cos t + C_4\sin t, \quad \dot{x}_2 = -C_2\sin t + C_4\cos t. \end{aligned} \qquad (4)$$

The second step is to define a coordinate transformation $x(t) = g(t, y(t))$ which has a topology (4) of the non-perturbed system (3)

$$\begin{aligned} x_1 &= y_1\cos t + y_3\sin t, \quad \dot{x}_1 = -y_1\sin t + y_3\cos t, \\ x_2 &= y_2\cos t + y_4\sin t, \quad \dot{x}_2 = -y_2\sin t + y_4\cos t. \end{aligned} \qquad (5)$$

The transformation (5) will result in the system of the standard form

$$\frac{dy}{dt} = \varepsilon Y(y, t) \qquad (6)$$

where $y = (y_1, y_2, y_3, y_4)$ and

$$Y(y,t) = J^{-1}Q(g(t,y)) = \begin{bmatrix} -\sin t & 0 \\ 0 & -\sin t \\ \cos t & 0 \\ 0 & \cos t \end{bmatrix} \begin{bmatrix} Q_1 \\ Q_2 \end{bmatrix}$$

Here J^{-1} is the inverse of the Jacobian of the transformation $x(t) = g(t, y(t))$.

The right-hand side of (6) is an explicit function of the state vector y and time t. Since the solution (4) of the non-perturbed equation (3) is periodic, time averaging formalism can be applied. This results in a simplified equation:

$$\frac{dy}{dt} = \varepsilon\overline{Y}(y) \qquad (7)$$

where

$$\overline{Y}(y) = \frac{1}{2\pi}\int_0^{2\pi} Y(y,t)\,dt$$

The procedure described in this section, transforms the original system into the normalized system (3), which after averaging is transformed to (7). The underlying theory of this method guarantees that the solution of the system (7) is close to the solution of (3). The new system (7) allows fast simulation of the long-term response (in the time-scale of the input angular velocity) of the non-ideal gyroscope.

ERROR CLASSIFICATION

The decomposition procedure described in the previous section makes the simulation of the long-term behavior of the gyroscope in presence of perturbations very computationally efficient. In this section, we qualitatively classify errors in vibratory gyroscopes based on the results of motion decomposition. Figure 5 summarizes gyroscope behavior in presence of imperfections.

Nominally, the gyroscope oscillates along the x-axis (Fig.5(a)). Spherical forces (diagonal stiffness matrix) cause only frequency change (Fig. 5(a, b)); the line of oscillation remains the same. The hyperbolic potential forces (positive-definite stiffness matrix), in addition to the frequency changes, result in a disruption of the straight line oscillation (Fig. 5(c, d)). Non-potential forces can appear only if off-diagonal elements in the stiffness matrix are not equal. They can appear, for example, as a side effect of the active control. These forces also cause disruption of the straight line oscillation, but do not result in frequency change (Fig. 5 (e, f)).

Asymmetry in damping can be presented in the form of dissipative spherical forces, dissipative hyperbolic forces, and gyroscopic forces. The dissipative spherical forces cause only amplitude changes (Fig. 5 (g,h)). Hyperbolic velocity dependent forces result in precession of the straight line oscillation and amplitude change (Figure 5 (k, l)). Gyroscopic forces can cause only precession (Figure 5 (m, n)). Dissipative spherical forces and hyperbolic forces can appear as result of losses due to structural damping, transmission of energy to suspension, aerodynamic drag, etc. Gyroscopic forces can appear only as inertial forces or as a side effect of the active control.

The most dangerous perturbations for the gyroscope operation are hyperbolic potential forces, non-potential forces, hyperbolic velocity dependent forces, and gyroscopic-like forces appearing as off-diagonal elements in the damping matrix.

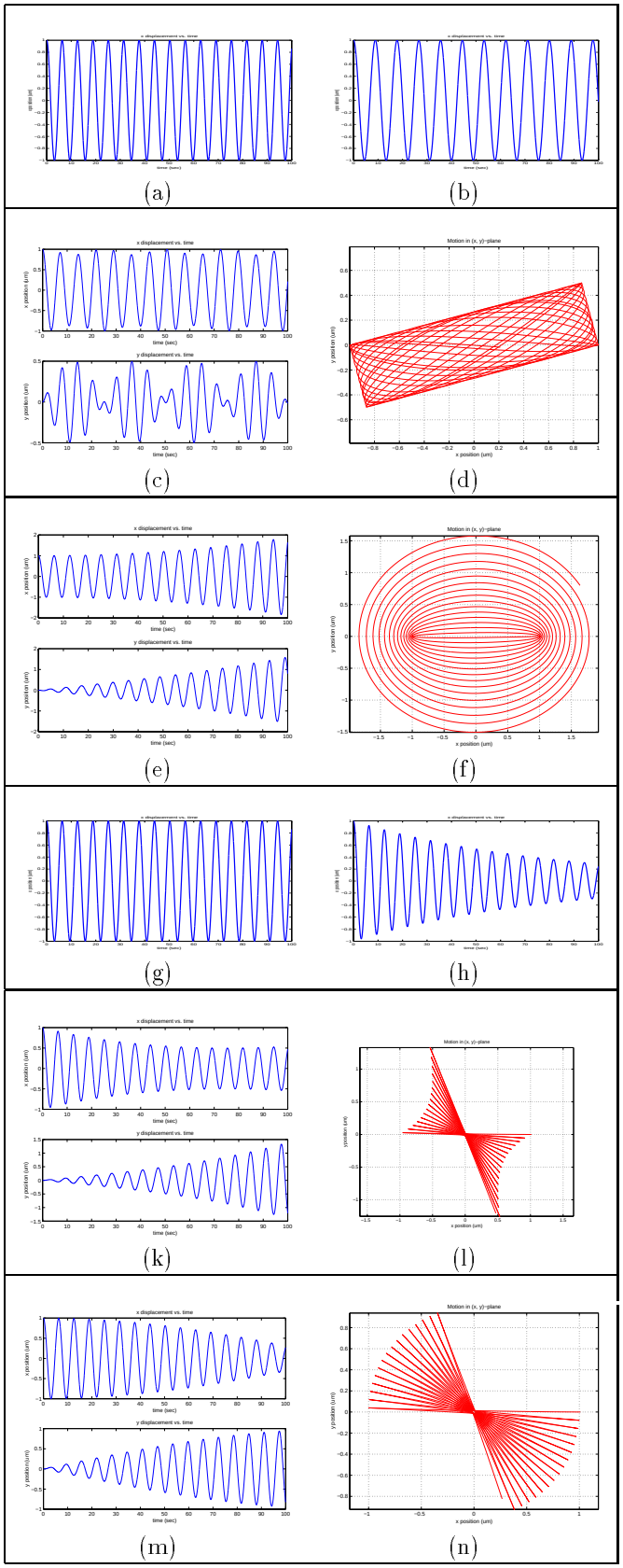

Figure 5: Classification of imperfections.

References

[1] Igor V. Novozhilov. *"Fractional Analysis: Methods of Motion Decomposition"*. Prentice-Hall, New York, 1995.

[2] Leonard Meirovitch. *"Principles and Techniques of Vibrations"*. Prentice-Hall, New York, 1997.

[3] Young-Ho Cho, Byung Man Kwak, Albert P. Pisano, and Roger T. Howe. Slide film damping in laterally driven microstructures. *Sensors and Actuators A*, 40:31–39, 1994.

[4] N. N. Bogolyubov and Yu. A. Mitropolsky. *"Asymptotic Methods in Theory of Nonlinear Oscillations"*. GIFML, Moscow, 1958. (in Russian).